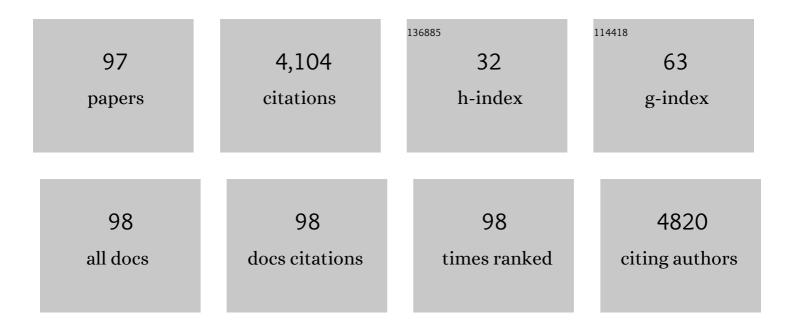
List of Publications by Year in descending order

Source: https://exaly.com/author-pdf/7323299/publications.pdf Version: 2024-02-01



#	Article	IF	CITATIONS
1	Multilayer Graphene Battery Anodes on Plastic Sheets for Flexible Electronics. ACS Applied Energy Materials, 2020, 3, 8410-8414.	2.5	10
2	Enhancement of the thermoelectric power factor by tuning the carrier concentration in Cu-rich and Ge-poor colusites Cu26+xNb2Ge6â ^{^2} xS32. Journal of Materials Chemistry C, 2020, 8, 6442-6449.	2.7	5
3	High-Electrical-Conductivity Multilayer Graphene Formed by Layer Exchange with Controlled Thickness and Interlayer. Scientific Reports, 2019, 9, 4068.	1.6	89
4	Three-step growth of highly photoresponsive BaSi2 light absorbing layers with uniform Ba to Si atomic ratios. Journal of Applied Physics, 2019, 126, .	1.1	16
5	Lithium-ion intercalation and deintercalation behaviors of graphitized carbon nanospheres. Journal of Materials Chemistry A, 2018, 6, 1128-1137.	5.2	28
6	Structure and solvents effects on the optical properties of sugar-derived carbon nanodots. Scientific Reports, 2018, 8, 6559.	1.6	121
7	Mechanism of Soot Oxidation over CeO2–ZrO2 under O2 Flow. Bulletin of the Chemical Society of Japan, 2018, 91, 437-443.	2.0	0
8	Metal Catalysts for Layer-Exchange Growth of Multilayer Graphene. ACS Applied Materials & Interfaces, 2018, 10, 41664-41669.	4.0	23
9	A carbonaceous two-dimensional lattice with FeN ₄ units. Chemical Communications, 2018, 54, 8995-8998.	2.2	8
10	Electrochemical Behavior of Graphitized Carbon Nanospheres in a Propylene Carbonate-Based Electrolyte Solution. Journal of the Electrochemical Society, 2018, 165, A2247-A2254.	1.3	4
11	Fabrication of SrGe2 thin films on Ge (100), (110), and (111) substrates. Nanoscale Research Letters, 2018, 13, 22.	3.1	1
12	Direct synthesis of multilayer graphene on an insulator by Ni-induced layer exchange growth of amorphous carbon. Applied Physics Letters, 2017, 110, .	1.5	26
13	Sandwichâ€Type Nanocomposite of Reduced Graphene Oxide and Periodic Mesoporous Silica with Vertically Aligned Mesochannels of Tunable Pore Depth and Size. Advanced Functional Materials, 2017, 27, 1704066.	7.8	14
14	Graphene Nanocomposites: Sandwichâ€īype Nanocomposite of Reduced Graphene Oxide and Periodic Mesoporous Silica with Vertically Aligned Mesochannels of Tunable Pore Depth and Size (Adv. Funct.) Tj ETQqO	0 07.gBT /0	Dveolock 10 Tf
15	High-quality multilayer graphene on an insulator formed by diffusion controlled Ni-induced layer exchange. Applied Physics Letters, 2017, 111, .	1.5	26
16	Silver-induced layer exchange for polycrystalline germanium on a flexible plastic substrate. Journal of Applied Physics, 2017, 122, .	1.1	16
17	Enhanced Durability of Porous Carbon/Single-Walled Carbon Nanotube Composite Electrodes for Supercapacitors. Journal of the Electrochemical Society, 2016, 163, A1753-A1758.	1.3	5
18	Orientation control of intermediate-composition SiGe on insulator by low-temperature Al-induced crystallization. Scripta Materialia, 2016, 122, 86-88.	2.6	14

#	Article	IF	CITATIONS
19	Nano- and Submicrometer-Sized Spherical Particle Fabrication Using a Submicroscopic Droplet Formed Using Selective Laser Heating. Journal of Physical Chemistry C, 2016, 120, 2439-2446.	1.5	46
20	Correlation between the pore structure and electrode density of MgO-templated carbons for electric double layer capacitor applications. Journal of Power Sources, 2016, 305, 128-133.	4.0	23
21	Transfer-free synthesis of highly ordered Ge nanowire arrays on glass substrates. Applied Physics Letters, 2015, 107, 133102.	1.5	6
22	Improved Surface Quality of the Metal-Induced Crystallized Ge Seed Layer and Its Influence on Subsequent Epitaxy. Crystal Growth and Design, 2015, 15, 1535-1539.	1.4	30
23	Electrochemical behavior of MgO-templated mesoporous carbons in the propylene carbonate solution of sodium hexafluorophosphate. Journal of Applied Electrochemistry, 2015, 45, 273-280.	1.5	6
24	Contribution of mesopores in MgO-templated mesoporous carbons to capacitance in non-aqueous electrolytes. Journal of Power Sources, 2015, 276, 176-180.	4.0	23
25	Effects of flexible substrate thickness on Al-induced crystallization of amorphous Ge thin films. Thin Solid Films, 2015, 583, 221-225.	0.8	9
26	70 °C synthesis of high-Sn content (25%) GeSn on insulator by Sn-induced crystallization of amorphous Ge. Applied Physics Letters, 2015, 106, .	1.5	64
27	Excellent Rate Capability of MgO-Templated Mesoporous Carbon as an Na-Ion Energy Storage Material. ECS Electrochemistry Letters, 2014, 4, A22-A23.	1.9	13
28	Selective formation of large-grained, (100)- or (111)-oriented Si on glass by Al-induced layer exchange. Journal of Applied Physics, 2014, 115, .	1.1	40
29	Quiescent hydrothermal synthesis of reduced graphene oxide–periodic mesoporous silica sandwich nanocomposites with perpendicular mesochannel alignments. Adsorption, 2014, 20, 267-274.	1.4	11
30	Direct synthesis of highly textured Ge on flexible polyimide films by metal-induced crystallization. Applied Physics Letters, 2014, 104, .	1.5	20
31	Synergetic photocatalysts derived from porous organo Ti–O clusters pillared graphene oxide frameworks (GOFs). RSC Advances, 2014, 4, 60729-60732.	1.7	5
32	Orientation control of Ge thin films by underlayer-selected Al-induced crystallization. CrystEngComm, 2014, 16, 2578.	1.3	17
33	Self-organization of Ge(111)/Al/glass structures through layer exchange in metal-induced crystallization. CrystEngComm, 2014, 16, 9590-9595.	1.3	10
34	Systematic changes in pore size distribution of template carbon obtained via chemical reaction between different cellulose precursors and halogens. Carbon, 2014, 77, 1191-1194.	5.4	2
35	Highly enhanced capacitance of MgO-templated mesoporous carbons in low temperature ionic liquids. Journal of Power Sources, 2014, 271, 377-381.	4.0	35
36	Orientation Control of Large-Grained Si Films on Insulators by Thickness-Modulated Al-Induced Crystallization. Crystal Growth and Design, 2013, 13, 1767-1770.	1.4	44

#	Article	IF	CITATIONS
37	Formation of polycrystalline BaSi2 films by radio-frequency magnetron sputtering for thin-film solar cell applications. Thin Solid Films, 2013, 534, 116-119.	0.8	32
38	Formation of large-grain-sized BaSi2 epitaxial layers grown on Si(111) by molecular beam epitaxy. Journal of Crystal Growth, 2013, 378, 193-197.	0.7	5
39	Large photoresponsivity in semiconducting BaSi2 epitaxial films grown on Si(001) substrates by molecular beam epitaxy. Journal of Crystal Growth, 2013, 378, 198-200.	0.7	4
40	Double-Layered Ge Thin Films on Insulators Formed by an Al-Induced Layer-Exchange Process. Crystal Growth and Design, 2013, 13, 3908-3912.	1.4	17
41	Large-Grained Polycrystalline (111) Ge Films on Insulators by Thickness-Controlled Al-Induced Crystallization. ECS Journal of Solid State Science and Technology, 2013, 2, Q195-Q199.	0.9	17
42	Effect of Ge/Al thickness on Al-induced crystallization of amorphous Ge layers on glass substrates. Physica Status Solidi C: Current Topics in Solid State Physics, 2013, 10, 1781-1784.	0.8	0
43	Epitaxial growth of BaSi2films with large grains using vicinal Si(111) substrates. Physica Status Solidi C: Current Topics in Solid State Physics, 2013, 10, 1756-1758.	0.8	1
44	Structure and texture of phenol-based carbon nanofibers heat-treated at high temperatures. Tanso, 2013, 2013, 110-115.	0.1	1
45	Epitaxy of Orthorhombic BaSi\$_{2}\$ with Preferential In-Plane Crystal Orientation on Si(001): Effects of Vicinal Substrate and Annealing Temperature. Japanese Journal of Applied Physics, 2012, 51, 095501.	0.8	15
46	Molecular Beam Epitaxy of BaSi\$_{2}\$ Films with Grain Size over 4 \$mu\$m on Si(111). Japanese Journal of Applied Physics, 2012, 51, 098003.	0.8	18
47	Highly (111)-oriented Ge thin films on insulators formed by Al-induced crystallization. Applied Physics Letters, 2012, 101, 072106.	1.5	88
48	Molecular beam epitaxy of BaSi2 thin films on Si(001) substrates. Journal of Crystal Growth, 2012, 345, 16-21.	0.7	61
49	Investigation of grain boundaries in BaSi2 epitaxial films on Si(1 1 1) substrates using transmission electron microscopy and electron-beam-induced current technique. Journal of Crystal Growth, 2012, 348, 75-79.	0.7	133
50	Graphitization behavior of carbon nanofibers derived from bacteria cellulose. Tanso, 2012, 2012, 225-230.	0.1	4
51	Acceleration of graphitization on carbon nanofibers prepared from bacteria cellulose dispersed in ethanol. Carbon, 2012, 50, 4757-4760.	5.4	12
52	Epitaxy of Orthorhombic BaSi2with Preferential In-Plane Crystal Orientation on Si(001): Effects of Vicinal Substrate and Annealing Temperature. Japanese Journal of Applied Physics, 2012, 51, 095501.	0.8	2
53	Molecular Beam Epitaxy of BaSi2Films with Grain Size over 4 µm on Si(111). Japanese Journal of Applied Physics, 2012, 51, 098003.	0.8	2
54	A sustainable synthesis of nitrogen-doped carbon aerogels. Green Chemistry, 2011, 13, 2428.	4.6	185

#	Article	IF	CITATIONS
55	Ordered Carbohydrate-Derived Porous Carbons. Chemistry of Materials, 2011, 23, 4882-4885.	3.2	136
56	Development and degradation of graphitic microtexture in carbon nanospheres under a morphologically restrained condition. Materials Chemistry and Physics, 2010, 121, 419-424.	2.0	16
57	Novel Graphitised Carbonaceous Materials for Use as a Highly Corrosionâ€₹olerant Catalyst Support in Polymer Electrolyte Fuel Cells. Fuel Cells, 2010, 10, 960-965.	1.5	8
58	MgO-templated nitrogen-containing carbons derived from different organic compounds for capacitor electrodes. Journal of Power Sources, 2010, 195, 667-673.	4.0	59
59	TEM and Electron Tomography Imaging of Pt Particles Dispersed on Carbon Nanospheres. Journal of Nano Research, 2010, 11, 119-124.	0.8	3
60	Hole Opening of Carbon Nanotubes and Their Capacitor Performance. Energy & Fuels, 2010, 24, 3373-3377.	2.5	39
61	Synthesis and Characteristics of Graphene Oxide-Derived Carbon Nanosheetâ^'Pd Nanosized Particle Composites. Langmuir, 2010, 26, 6681-6688.	1.6	62
62	Fabrication and characterization of mesoporous carbon nanosheets-1D TiO2 nanostructures. Journal of Materials Chemistry, 2010, 20, 2424.	6.7	21
63	Debundling of SWCNTs through a simple intercalation technique. Electrochemistry Communications, 2009, 11, 1441-1444.	2.3	11
64	Enhanced Hydrogen Adsorptivity of Single-Wall Carbon Nanotube Bundles by One-Step C ₆₀ -Pillaring Method. Nano Letters, 2009, 9, 3694-3698.	4.5	35
65	TEM observation of heterogeneous polyhedronization behavior in graphitized carbon nanospheres. Materials Science and Engineering B: Solid-State Materials for Advanced Technology, 2008, 148, 245-248.	1.7	16
66	Lamellar carbon nanosheets function as templates for two-dimensional deposition of tubular titanate. Chemical Communications, 2008, , 4348.	2.2	24
67	Property of upgraded solid product from low rank coal by thermal reaction with solvent. Fuel Processing Technology, 2007, 88, 333-341.	3.7	8
68	TEM and electron tomography studies of carbon nanospheres for lithium secondary batteries. Carbon, 2006, 44, 2558-2564.	5.4	56
69	Formation of graphite-derived layered mesoporous carbon materials. Microporous and Mesoporous Materials, 2006, 93, 254-262.	2.2	1
70	Dependence of microscopic structure and swelling property of DTF chars upon heat-treatment temperature. Fuel, 2006, 85, 2064-2070.	3.4	29
71	XRD analysis of carbon stacking structure in coal during heat treatment. Fuel, 2004, 83, 2427-2433.	3.4	350
72	Adsorptive hydrogen storage in carbon and porous materials. Materials Science and Engineering B: Solid-State Materials for Advanced Technology, 2004, 108, 143-147.	1.7	154

#	Article	IF	CITATIONS
73	Structure of porous carbon materials for energy storage applications. Ganseki Kobutsu Kagaku, 2004, 33, 114-120.	0.1	0
74	Preparation and pore control of highly mesoporous carbon from defluorinated PTFE. Carbon, 2003, 41, 1759-1764.	5.4	77
75	Structure and electrochemical properties of carbon aerogels polymerized in the presence of Cu2+. Journal of Non-Crystalline Solids, 2003, 330, 99-105.	1.5	50
76	Tem Observation of Metal-Loaded Carbon Aerogels Prepared by an Ion-Exchange Method. Molecular Crystals and Liquid Crystals, 2002, 388, 75-80.	0.4	2
77	Preparation and Characterization of Porous Carbons By Defluorination of Ptfe with Alkali Metals - Effect of Alkali Metals on the Porous Structure Molecular Crystals and Liquid Crystals, 2002, 388, 45-50.	0.4	10
78	Surface-Enhanced Raman Spectroscopy in Single Living Cells Using Gold Nanoparticles. Applied Spectroscopy, 2002, 56, 150-154.	1.2	559
79	XPS Study of Copper-Doped Carbon Aerogels. Langmuir, 2002, 18, 10100-10104.	1.6	89
80	Synthesis and Characterization of Copper-Doped Carbon Aerogels. Langmuir, 2002, 18, 7073-7076.	1.6	119
81	XRD evaluation of KOH activation process and influence of coal rank. Fuel, 2002, 81, 1717-1722.	3.4	94
82	Structural changes in carbon aerogels with high temperature treatment. Carbon, 2002, 40, 575-581.	5.4	123
83	Mesoporous carbon from poly(tetrafluoroethylene) defluorinated by sodium metal. Carbon, 2002, 40, 457-459.	5.4	29
84	Preparation of Porous Carbon by Defluorination of Poly(tetrafluoroethylene) and the Effect of Î ³ -Irradiation on the Polymer. Chemistry of Materials, 2001, 13, 2933-2939.	3.2	31
85	The Structures of Copper-Doped Carbon Aerogels Prepared by an Ion Exchange Method. Materials Research Society Symposia Proceedings, 2001, 697, 8281.	0.1	1
86	Flow behavior of graphitized carbon black suspensions. Carbon, 2001, 39, 2384-2386.	5.4	7
87	Title is missing!. Journal of Materials Science, 2001, 36, 4249-4257.	1.7	20
88	XRD evaluation of CO2 activation process of coal- and coconut shell-based carbons. Fuel, 2000, 79, 1461-1466.	3.4	84
89	The modification of pore size in activated carbon fibers by chemical vapor deposition and its effects on molecular sieve selectivity. Carbon, 1998, 36, 377-382.	5.4	61
90	The Pore Structure Determination of Carbon Aerogels. Adsorption, 1998, 4, 187-195.	1.4	77

#	Article	IF	CITATIONS
91	Title is missing!. Journal of Materials Science, 1998, 33, 199-206.	1.7	44
92	Coal-Based Activated Carbons Prepared with Organometallics and Their Mesoporous Structure. Energy & Fuels, 1997, 11, 327-330.	2.5	43
93	Evaluation of accessible and inaccessible microporosities of microporous carbons. Journal of the Chemical Society, Faraday Transactions, 1996, 92, 2297.	1.7	20
94	Transition process to diamond from C60 fullerene. Chemical Physics Letters, 1994, 226, 595-599.	1.2	7
95	Amorphous diamond from C60fullerene. Applied Physics Letters, 1994, 64, 1797-1799.	1.5	104
96	Structure of amorphous hydrogenated carbon film prepared from rf plasma deposition. Carbon, 1993, 31, 1049-1055.	5.4	12
97	Microtexture of High Surface Area Activated Carbons. Tanso, 1992, 1992, 295-300.	0.1	6